MOLECULAR AND CELLULAR BIOLOGY, Feb. 1999, p. 1498–1507 Vol. 19, No. 2
0270-7306/99/$04.00+0

rlk/*TXK* Encodes Two Forms of a Novel Cysteine String Tyrosine Kinase Activated by Src Family Kinases

JAYANTHA DEBNATH,[1,2,3]† MARIO CHAMORRO,[1,4] MICHAEL J. CZAR,[3] EDWARD M. SCHAEFFER,[2,3] MICHAEL J. LENARDO,[5] HAROLD E. VARMUS,[1] AND PAMELA L. SCHWARTZBERG[1,3]*

National Cancer Institute,[1] Howard Hughes Medical Institute—NIH Research Scholars Program,[2] National Institute for Human Genome Research,[3] and National Institute of Allergy and Infectious Diseases,[5] National Institutes of Health, Bethesda, Maryland, and George Washington Institute of Biomedical Sciences, Washington, D.C.[4]

Received 20 February 1998/Returned for modification 14 April 1998/Accepted 30 October 1998

Rlk/Txk is a member of the BTK/Tec family of tyrosine kinases and is primarily expressed in T lymphocytes. Unlike other members of this kinase family, Rlk lacks a pleckstrin homology (PH) domain near the amino terminus and instead contains a distinctive cysteine string motif. We demonstrate here that Rlk protein consists of two isoforms that arise by alternative initiation of translation from the same cDNA. The shorter, internally initiated protein species lacks the cysteine string motif and is located in the nucleus when expressed in the absence of the larger form. In contrast, the larger form is cytoplasmic. We show that the larger form is palmitoylated and that mutation of its cysteine string motif both abolishes palmitoylation and allows the protein to migrate to the nucleus. The cysteine string, therefore, is a critical determinant of both fatty acid modification and protein localization for the larger isoform of Rlk, suggesting that Rlk regulation is distinct from the other Btk family kinases. We further show that Rlk is phosphorylated and changes localization in response to T-cell-receptor (TCR) activation and, like the other Btk family kinases, can be phosphorylated and activated by Src family kinases. However, unlike the other Btk family members, Rlk is activated independently of the activity of phosphatidylinositol 3-kinase, consistent with its lack of a PH domain. Thus, Rlk has two distinct isoforms, each of which may have unique properties in signaling downstream from the TCR.

The initiation of signal transduction through antigen receptors in lymphocytes is associated with the rapid sequential activation of a number of tyrosine kinases, including well-studied members of the Src and the ZAP-70/Syk families (35). However, in B cells, a third nonreceptor tyrosine kinase, Btk, is also important for signaling from antigen and other lymphocyte cell surface receptors (4). Mutations in *btk* result in a severe B-cell immunodeficiency, X-linked agammaglobulinemia (XLA), and the murine counterpart X-linked immunodeficiency (*xid*), characterized by decreased mature B-cell and immunoglobulin levels. Btk kinase activity and tyrosine phosphorylation have both been shown to increase upon cross-linking or stimulation of surface immunoglobulin M and the interleukin 5 (IL-5) and IL-6 receptors in B cells, as well as cross-linking of the high-affinity immunoglobulin E receptor (FcεRII) in mast cells (15, 24, 29, 30). Another Btk family kinase, Itk, which is expressed in T cells, is tyrosine phosphorylated and activated by engagement of either the T-cell receptor (TCR) or CD28 in T-cell lines and by FcεRII stimulation in mast cells (1, 6, 16).

The Btk family kinases have a modular structure including the kinase and SH2 and SH3 protein interaction domains, as well as a proline-rich region and a pleckstrin homology (PH) domain. Examination of lymphocyte signaling suggests that Btk family members function downstream of Src family kinases. Src family kinases have been shown to phosphorylate Btk family members on a tyrosine in the activation loop of the kinase domain leading to kinase activation and, for Btk, autophosphorylation of a site in the SH3 domain (10, 22, 26). The activation of Btk and Itk by Src family kinases is both potentiated by and dependent on an interaction between the PH domains of the Btk kinases and the products of phosphatidylinositol (PI) 3-kinase (2, 19), demonstrating the importance of the PH domain in these signaling pathways.

rlk/*TXK*, originally isolated in screens for genes encoding tyrosine kinases from both human peripheral blood and murine embryonic thymus, encodes a kinase that closely resembles members of the Btk/Tec family (9, 12, 32). Rlk shares with Btk kinases the proline-rich motif and homologous SH3, SH2, and kinase domains, including the tyrosine phosphorylation sites in the SH3 and kinase sequences (Fig. 1). However, unlike the other Btk family members, Rlk lacks a PH domain and instead possesses a distinctive cysteine string motif, suggesting that Rlk has a unique role in TCR signaling. Like Itk, Rlk is specifically expressed in developing and mature T cells as well as mast cells. However, little is known about Rlk protein function in the T cell. Evidence from our and other laboratories suggests that Rlk and Itk together have important roles in signaling from the TCR—targeted mutations of either kinase cause only mild defects in T-cell numbers and decreased cytokine production (20, 21). However, mutation of both kinases leads to profound defects in TCR-based signaling (unpublished data).

In order to characterize Rlk/Txk biochemically, we examined properties of endogenous Rlk in T cells and Rlk-green fluorescent protein (GFP) constructs expressed in the Jurkat T-cell lymphoma cell line and in heterologous cells. We demonstrate here that Rlk consists of two protein species generated by alternative initiation of translation. These two species have distinct properties and subcellular localizations that are

* Corresponding author. Mailing address: National Human Genome Research Institute, 49/4A38, National Institutes of Health, Bethesda, MD 20892-4472. Phone: (301) 435-1906. Fax: (301) 402-2170. E-mail: pams@nhgri.nih.gov.

† Present address: Department of Pathology, Brigham and Women's Hospital, Boston, MA 02115.

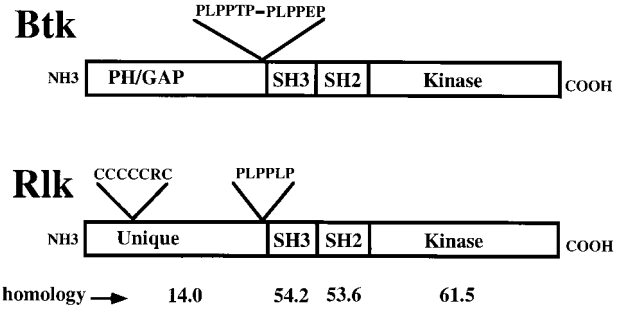

FIG. 1. Comparison of the predicted organizations of Rlk and Btk. Percent amino acid identities are indicated at the bottom of the figure.

dictated by the presence of a cysteine string motif, which is an essential requirement for palmitoylation of the full-length protein. Coexpression of Rlk and Src family members leads to the tyrosine phosphorylation and kinase activation of Rlk. However, unlike for Btk and Itk, phosphorylation of Rlk does not appear to require PI 3-kinase activity, consistent with the lack of a PH domain. Activation of the Jurkat T-cell lymphoma line through the TCR increases tyrosine phosphorylation of transiently transfected Rlk and can lead to alterations in Rlk subcellular localization, suggesting that the nuclear localization of Rlk may play an important role in its normal function. Thus, despite lacking the PH domain, Rlk can act as a substrate for Src family kinases and may participate in novel signal transduction pathways downstream of the TCR.

MATERIALS AND METHODS

Cell culture and transfection. 293T cells were a generous gift from the laboratory of D. Baltimore (Massachusetts Institute of Technology). 293T and HeLa cells were maintained in Dulbecco's modified Eagle's medium supplemented with 10% fetal calf serum, penicillin, streptomycin, and 10 mM glutamine. Jurkat cells expressing simian virus 40 large T antigen (Tag) were a generous gift from Gerald Crabtree (Stanford University). Jurkat and Jurkat Tag cell lines were maintained in RPMI 1640 supplemented with 10% fetal calf serum, penicillin, streptomycin, glutamine, and 50 μM 2-mercaptoethanol.

Antibodies and reagents. Anti-murine Rlk was raised in rabbits against a glutathione *S*-transferase (GST) fusion protein containing the predicted amino terminus and SH3 domain of full-length murine Rlk (residues 1 to 138). DNA sequences encoding residues 1 to 138 of full-length Rlk were amplified by PCR and fused in frame to pGEX-4T (Pharmacia). GST fusion proteins were grown in bacterial strain BL21Plys5 at 37°C and induced with 100 mM IPTG (isopropyl-β-D-thiogalactopyranoside) at 25°C for 2 h. Proteins were separated by sodium dodecyl sulfate-polyacrylamide gel electrophoresis (SDS-PAGE), lightly stained with Coomassie blue, eluted from the gel into 0.1% SDS–0.1 M Tris (pH 8.0), and used to immunize rabbits (Assay Research Co., College Park, Md.). The antisera were affinity purified by incubation of 1-ml aliquots of whole serum with nitrocellulose strips containing the GST fusion protein overnight in 50 ml of phosphate-buffered saline (PBS), elution with 1 ml of 25 mM glycine (pH 3.3), and resuspension in 5 ml of Tris-HCl (pH 8.0) with 1% bovine serum albumin (fraction V; Sigma).

Anti-TXK serum was a generous gift from M. Tomlinson (DNAX). OKT3 was a generous gift from A. Weissman (National Institutes of Health [NIH], Bethesda, Md.). Anti-Fyn (FYN3) serum was purchased from Santa Cruz Biochemicals (Santa Cruz, Calif.), antiphosphotyrosine (4G10) was purchased from Upstate Biotechnology (Lake Placid, N.Y.), anti-Myc (9E10) was purchased from Boehringer Mannheim (Indianapolis, Ind.), and anti-FLAG monoclonal antibody M2 was purchased from Kodak (Rochester, N.Y.).

Constructs and mutagenesis. A fragment of mouse Rlk cDNA was subcloned into pCI (Invitrogen) by using an *Msc*I site near the 5′ end of the cDNA and an *Xho*I site at the 3′ end. An *myc* epitope tag was introduced by inserting an oligonucleotide encoding the 15-amino-acid Myc tag from the *Bst*EII site at the stop codon of Rlk to the downstream *Afl*II site. The *myc*-tagged cDNA was also transferred into pcDNA3 with an *Nhe*I-to-*Xho*I fragment. The amino-terminal deletion mutant Δ54 was generated by deleting from the *Nhe*I site to the *Bst*XI site in pCIRlk. Rlk-GFP was generated by inserting a linker containing a *Bst*EII site from the *Sac*I site to the *Nhe*I site of pFRED25 (a generous gift of G. Gaitanairis and G. Pavlakis, NCI-ABL, Frederick, Md.). A *Bst*EII-to-*Xba*I fragment of the modified pFRED25 containing the GFP coding sequences was subcloned onto the *Bst*EII site at the stop codon of Rlk subclone pCIR (12). pCEF was a gift of Silvio Gutkind (NIH). pCEF-Rlk was generated by subcloning Rlk-GFP into pCEF by three-fragment ligation with the *Eco*RI, *Asp*718, and *Not*I sites.

Point mutations were introduced into Rlk by a PCR-based strategy (11) and then subcloned into pcDNARlk. Mutagenesis was carried out by using the following oligonucleotides, with boldface type representing altered residues: AUG1 (GCA AGC AGG GTC GTC **TA**G ATC CTG TCC TCT); AUG2 (TGG TTC GCC AAG CTG **TT**G GGC AAA ACT CAA); CA2.1 (TGG TTC GCC AAG C**TT TT**G GGC AAA ACT CAA); NLS (GTG CAA CCT TCG AA**T AA**C AA**T** CCG CTG CCC CC); CYS (GTT CTC TGC TGC T**CG** T**CT** **GCG** CGC TGC TCA GTA CAG). The double-mutant DM was generated by introducing the CA2.1 mutation by PCR-based mutagenesis into the AUG1 construct. Mutations AUG1 and AUG2 were transferred to the Rlk-GFP fusions by subcloning with *Eco*NI and *Xba*I. The Rlk-BFP construct was generated by transferring an *Nhe*I-to-*Xba*I fragment containing BFP from pFRED-Blue (a gift of G. Gaitanairis and G. Pavlakis). All mutations were confirmed by dideoxy sequencing.

A phage clone containing human TXK was generously provided by Gary Littman (University of South Florida). The cDNA was recovered by an *Eco*RI digest and subcloned into the pCDNA3 expression vector (Invitrogen). pLNCX Fyn T was a generous gift from Cliff Lowell (USCF). Itk-FLAG was a generous gift of Littman (New York University, New York).

Transfections. Constructs were introduced into 293T cells by calcium phosphate transfection in media containing 25 μM chloroquine (Sigma) (25). Three to five micrograms of each plasmid was used for each transfection (2×10^6 cells); the cells were harvested 24 to 36 h later. Alternatively, cells were split 24 h after infection and treated 24 h later with either Wortmannin (1 μm), Ly294002 (100 μM), or carrier (dimethyl sulfoxide) for 30 min before harvest. Transfections into HeLa cells were performed identically, without the addition of chloroquine.

Jurkat and Jurkat Tag cell lines (10^7 cells) were electroporated with 25 to 40 μg of the appropriate DNA with a Bio-Rad electroporator at 250 V and 960 μF. Cells were harvested 24 h later.

In vitro translation. In vitro translation employed the TnT coupled reticulocyte lysate system (Promega); 1 μg of each construct was used for each reaction at 30°C for 1 h with 20 μCi of [^{35}S]methionine (1,000 Ci/mmol) (Redivue; Amersham). Translation products were separated by SDS–10% PAGE, soaked in Enlighten (NEN), dried, and analyzed by fluorography.

Western blotting and immunoprecipitation. Cells were harvested 24 h following transfection. Cells were washed once with ice-cold PBS and lysed in ice-cold Nonidet P-40 (NP-40) lysis buffer (0.5% NP-40, 50 mM HEPES [pH 7.4], 5 mM EDTA, 50 mM NaCl, 10 mM $NaPO_4$, 50 mM NaF, 1 mM sodium orthovanadate, 1 mM AEBSF, 2 U of aprotinin per ml) for 10 min on ice. Total protein extracts were mixed directly with 2× SDS protein sample buffer (1× SDS protein sample buffer is 50 mM Tris [pH 6.8], 2% SDS, 10% glycerol, and 0.1% bromphenol blue plus 5% β-mercaptoethanol). Alternatively, lysates were clarified by centrifugation and detergent-soluble protein was analyzed. Equivalent amounts of protein were boiled in SDS sample buffer and separated by SDS–10% PAGE and transferred to nitrocellulose (Schleicher and Schuell). The membranes were blocked in TBST (10 mM Tris-HCl [pH 8.0], 150 mM NaCl, 0.1% Tween 20) with 5% (wt/vol) nonfat dry milk and incubated with the appropriate primary antibody at a 1:2,000 (anti-Rlk and 4G10 [antiphosphotyrosine]) or 1:1,000 (anti-Fyn) dilution overnight at 4°C for 1 to 2 h at room temperature. Membranes were washed and incubated with the appropriate secondary antibody at a 1:10,000 dilution (Boehringer Mannheim) for 1 h, and protein was visualized by enhanced chemiluminescence (Amersham).

For immunoprecipitation and coimmunoprecipitation studies, equivalent amounts of detergent-soluble protein were incubated with affinity-purified anti-Rlk sera for 2 to 4 h at 4°C. The complexes were recovered with protein A-Sepharose (Sigma), washed two times with ice-cold NP-40 wash buffer (1% NP-40 in PBS, 1 mM sodium orthovanadate), and analyzed by Western blotting with either anti-Rlk or anti-Fyn antisera (1:1,000).

In vitro kinase assays. Cell extracts were prepared in NP-40 lysis buffer and immunoprecipitated as described above. Complexes were recovered with protein A-Sepharose, washed twice with ice-cold NP-40 wash buffer, and washed twice with ice-cold Rlk kinase buffer (30 mM HEPES [pH 7.4], 150 mM NaCl, 5 mM $MgCl_2$, 5 mM $MnCl_2$, 100 μM sodium orthovanadate). The kinase reaction was carried out in kinase buffer supplemented with 1 μg of acid-denatured enolase and 10 μCi of [γ-^{32}P]ATP (Redivue; Amersham) for 5 min at room temperature. The reaction was quenched with SDS sample buffer, boiled, and separated by SDS–10% PAGE. Phosphorylated proteins were detected by autoradiography or quantified on a PhosphorImager. The level of Rlk protein was measured by Western blotting. For in vitro kinase assay of Rlk derived from murine thymocytes, 10^7 cells were lysed in 1 ml of NP-40 lysis buffer and kinase assays were performed in a buffer containing 50 mM HEPES (pH 7.0), 150 mM NaCl, 10 mM dithiothreitol (DTT), 0.01% Brij 35, and 1 mM sodium orthovanadate. Assays were initiated by adding 50 mM $MgCl_2$ and 133 μCi of [γ-^{32}P]ATP (ICN), and mixtures were incubated for 20 min at room temperature. Assays were terminated by two washes with ice-cold NP-40 wash buffer plus 0.1% SDS and resuspension in 1× SDS protein sample buffer.

Subcellular fractionation of lymphocytes. Thymocytes (6×10^7) from C57BL/6 mice were swollen and dounced 20 times in homogenization buffer (10 mM HEPES [pH 7.0], 10 mM KCl, 1.5 mM $MgCl_2$, 1 mM EDTA, 1 mM DTT, and 1 mM Na_3VO_4 plus aprotinin, leupeptin, and AEBSF). The crude nuclear

pellet was obtained by spinning at 600 × *g* for 10 min at 4°C. A crude mitochondrial pellet was obtained from supernatant spun at 15,000 × *g* for 10 min at 4°C. The supernatant was spun at 100,000 × *g* for 60 min and was used as the cytoplasmic compartment. The pellets were resuspended in NP-40 lysis buffer at 37°C for 5 min and then placed at 4°C for 15 min and cleared at 15,000 × *g* for 10 min at 4°C. The S100 fraction was adjusted to 1× NP-40 lysis buffer, and immunoprecipitations and kinase assays were performed as described above.

Immunofluorescence. HeLa or 293T cells were transfected with Rlk expression constructs, passed onto coverslips 20 h later, and, 12 to 24 h later, fixed with 1% paraformaldehyde for 20 min at room temperature. Cells were washed in PBS and permeabilized with 0.1% Triton in PBS for 5 min at room temperature. Cells were then washed in PBS followed by H_2O, counterstained with DAPI (4′,6-diamidino-2-phenylindole) or propidium iodide, and visualized with a charge-coupled device camera on a Zeiss Axioplan microscope. Alternatively, Jurkat Tag cells were electroporated with pCEF Rlk-GFP and 24 h later divided into equal aliquots and left unstimulated or stimulated with either OKT3 or phorbol myristate acetate (PMA) at 20 ng/ml and ionomycin at 1 μg/ml. Cells were either examined live at sequential time points after stimulation or harvested, fixed, and counterstained with propidium iodide.

Metabolic labeling with [^{3}H]palmitate. Cells were transfected with Rlk expression constructs and incubated 36 h later in 1.5 ml of medium containing 5% dialyzed serum and 400 to 500 μCi of [^{3}H]palmitate per 6-cm dish. One to 3 h later, cells were lysed and Rlk was immunoprecipitated as described above. Low-reducing protein sample buffer with 20 mM DTT was used in these experiments, and samples were incubated at 65°C for 3 min prior to loading on SDS–10% polyacrylamide gels. Gels were soaked in En^{3}Hance (NEN), dried, and visualized by fluorography.

RESULTS

***rlk* encodes two protein species.** The *rlk* gene is expressed in the T-cell lineage, where its mRNA is down-regulated upon activation (12, 32). However, very little is known about the Rlk protein. To facilitate studies of Rlk, we generated antisera directed against a GST fusion protein containing the predicted amino-terminal 138 amino acids of Rlk, including the SH3 domain. We also extended the 3′ end of the *rlk* cDNA with a 45-nucleotide sequence encoding an *myc* epitope for expression studies in vitro and in cell culture.

The predicted amino acid sequence of Rlk encodes a protein of approximately 58 kDa. However, immunoprecipitation from extracts of murine thymocytes, splenocytes, and lymph node cells with our antibody, followed by in vitro kinase assays to detect autophosphorylation activity, revealed two major phosphorylated species of approximately 58 and 52 kDa (Fig. 2A, lanes 1 to 3). The two Rlk proteins were observed at various ratios (approximately 1:1) and were not detected when immunoprecipitation was performed with preimmune sera (Fig. 2B, lane 4) or in extracts from lymphocytes from mice homozygous for a targeted disruption of the *rlk* gene (30a). These observations suggest that the two proteins are both encoded by the Rlk gene.

To understand the nature of these two protein species, we expressed the full-length *myc*-tagged cDNA in 293T cells. We again observed two major protein species that migrated slightly slower than endogenous Rlk in T cells, as expected from the 15-amino-acid tag (Fig. 2B; compare lanes 2 and 3). The two protein species were observed by immunoprecipitation with either antibody directed against the predicted amino-terminal and SH3 domains or anti-*myc* monoclonal antibody directed against the COOH-terminal tag (data not shown); by immunoprecipitation-kinase assay (Fig. 2B, lane 3); or by direct Western analysis with the same antibodies (Fig. 2B, lane 6). The generation of two isoforms by a single cDNA suggested that the two forms of Rlk are encoded by a single mRNA species, and the recognition of both forms of Rlk by the anti-*myc* epitope antibody implied that these two forms share a common carboxy terminus.

Finally, in vitro-coupled transcription and translation of the full-length *myc*-tagged Rlk cDNA also revealed two major protein species migrating at positions expected for proteins of 59 and 53 kDa (Fig. 2B, lane 7). Similarly, in vitro transcription and translation, as well as transfection into 293T cells of full-length human *TXK* cDNA also generated two protein products, migrating as 58- and 55-kDa proteins (Fig. 2C, lane 2). The generation of two forms from both the mouse and human cDNAs suggested that the mechanism for synthesis of two Rlk/Txk isoforms from a single mRNA is conserved between these two species.

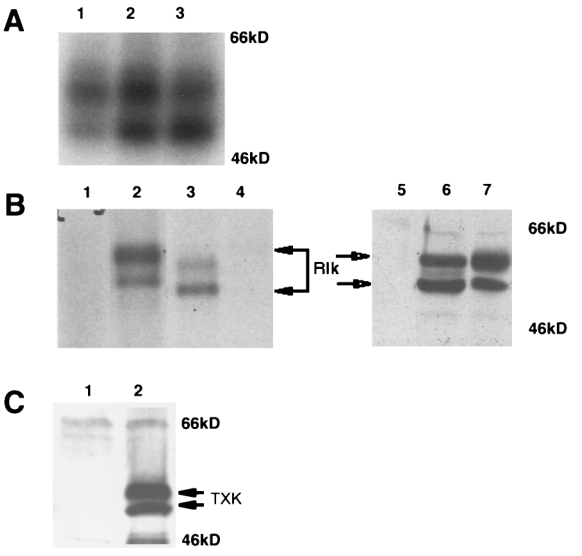

FIG. 2. Rlk encodes two proteins. (A) In vitro protein kinase assay of Rlk protein immunoprecipitated with anti-Rlk antiserum from lysates of murine lymph node cells (lane 1), splenocytes (lane 2), or thymocytes (lane 3). Immune complexes were labeled with [γ-^{32}P]ATP, resolved by SDS-PAGE, and visualized by autoradiography. (B) (Lanes 1 to 4) In vitro protein kinase assay of Rlk protein immunoprecipitated with anti-Rlk antiserum from lysates of 293T cells transfected with vector alone (lane 1) or murine *myc*-tagged *rlk* cDNA (lane 2) compared with immunoprecipitates from murine thymocytes (lane 3). Lane 4 contains immunoprecipitates with preimmune sera from thymocyte lysates. The two major protein species generated from the Rlk-*myc* construct migrate slightly slower than endogenous Rlk in T cells, as expected from the 15-amino-acid tag (lanes 3 and 2). Versions of the *rlk* cDNA lacking the *myc* insert generated proteins that comigrated with the endogenous forms (data not shown). (Lanes 5 to 7) Immunoblot analysis with anti-Rlk of 293T cell lysates from cells that were mock transfected (lane 5) or transfected with murine *rlk* cDNA (lane 6) compared to in vitro transcription-translation products (lane 7) generated from *rlk* cDNA. (C) Immunoblot analysis with anti-human TXK antisera of 293T cell lysates from cells that were mock transfected (lane 1) or transfected with human *Txk* cDNA (lane 2). The expected TXK products are indicated.

Murine and human *rlk*/*txk* genes contain internal initiation ATG codons. The production of two proteins from a single mouse or human *rlk*/*txk* cDNA in vivo and in vitro suggests that a posttranscriptional mechanism, such as protein processing or alternative translational initiation, is responsible for production of the second species. The results with in vitro translation, however, argue against proteolytic processing of the 58- to the 52-kDa form. Furthermore, pulse-chase analyses were also inconsistent with a precursor-product relationship for the 58- and 52-kDa species (data not shown). Examination of the *rlk* open reading frame revealed downstream in-frame ATGs that are embedded within efficient translation initiation consensus sequences in both the mouse and human cDNAs (17) and would be predicted to generate the shorter species (52 and 55 kDa in mice and humans, respectively [Fig. 3A]). Interestingly, these shorter Rlk open reading frames are predicted to lack the cysteine string motif that is unique to this tyrosine kinase.

Mutational analysis of putative translation start sites in murine *rlk*. To address whether alternative initiation codons were used, we generated mutations affecting the first ATG, the second ATG, or both (Fig. 3). The resulting mutant cDNAs

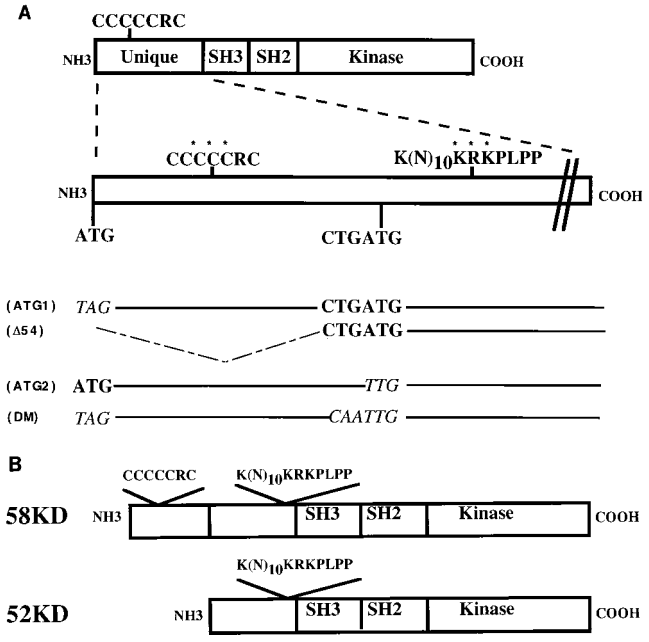

FIG. 3. Schematic of Rlk mutants. (A) Rlk protein organization and locations of the cysteine string motif and putative NLS in the amino terminus of Rlk. Residues changed in the mutants of the cysteine string motif and NLS are marked by asterisks. The relative positions of the putative translational initiation sites, as well as the nucleotide sequences of the various start site mutant derivatives (italicized), are shown below the schematic. SH3, Src homology 3; SH2, Src homology 2. (B) Schematic organization of the two forms of Rlk.

were assayed in vitro by using rabbit reticulocyte lysates and in transfected 293T cells.

Mutations that altered the first ATG included a change to TAG (ATG1) and a 54-codon deletion from the first ATG to a site just upstream of the second ATG (Δ54) (Fig. 3). These mutations abolished synthesis of the larger (58-kDa) protein product and augmented production of the 52-kDa protein both in vitro and in 293T cells (Fig. 4). This observation is consistent with the ribosome scanning model, in which removal of the upstream ATG leads to more efficient translation from the downstream ATG codon (17, 18). Since no other upstream ATG exists in our cDNA clones, these data also support the idea that the most 5′ ATG initiates translation of the larger protein and that the smaller protein is generated by translation from an internal start site, not by amino-terminal processing of the larger protein.

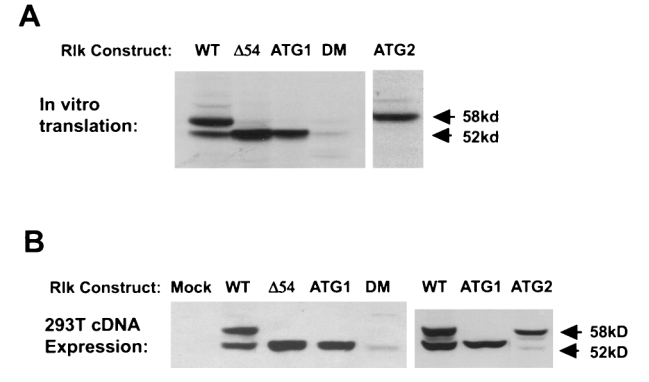

FIG. 4. Distinct protein isoforms of *rlk* are generated by the utilization of alternative translational start codons. (A) In vitro transcription-translation products generated from WT and mutant *rlk* cDNAs, resolved by SDS-PAGE, and visualized by fluorography. (B) Expression of *rlk* WT and mutant cDNAs in 293T cells. Equal amounts of protein from total cellular lysates of cells transfected with the indicated constructs were resolved by SDS-PAGE and visualized by immunoblotting with anti-Rlk serum (lower). Mutants are described in Fig. 3.

We next altered the ATG at codon 55 to TTG (ATG2) (Fig. 3). This mutation eliminated synthesis of the shorter (52-kDa) protein in vitro and drastically reduced its production in 293T cells (Fig. 4B). A double mutation (CA2) of both the internal ATG and an adjacent CTG gave similar results (data not shown). To determine whether this small amount of the 52-kDa Rlk protein may be generated by posttranslational cleavage in 293T cells, we engineered a mutant (DM) in which the first ATG and the internal ATG and CTG were all altered. Expression of DM in 293T cells still demonstrated a small residual amount of protein migrating similarly to the shorter form (Fig. 4B, lane 5). Since no larger Rlk protein is generated by this mutant, generation of a smaller protein could not result from posttranslation cleavage of the larger protein product. Based on these results, we conclude that the two Rlk isoforms arise by the alternative initiation of translation, with most of the 52-kDa form produced from an internal ATG codon at position 55.

The two RLK isoforms localize to different subcellular compartments. Analyses of extracts of cells that expressed the individual forms of the Rlk proteins suggested that there were differences in the detergent solubility of the two forms. In particular, the larger (58-kDa) form was relatively insoluble in nonionic detergents, suggesting that the two forms may localize to different subcellular compartments when produced separately.

To examine subcellular localization, we fused GFP to the carboxyl termini of the two products of wild-type (WT) *rlk* as well as to the products of the ATG1 and ATG2 alleles. Transient transfection of the Rlk-GFP fusion constructs generated the predicted 83- and 77-kDa fusion proteins that were kinase active and behaved like WT Rlk (for example, see Fig. 9). HeLa cells transiently transfected with the different Rlk-GFP constructs were fixed, stained with DAPI, and observed by fluorescence microscopy. Identical results were obtained with unfixed cells expressing Rlk-GFP and with cells expressing nontagged versions of Rlk examined by indirect immunofluorescence using anti-Rlk antisera (data not shown).

In HeLa cells, the WT Rlk-GFP construct, expressing both the 83- and 77-kDa proteins, showed a granular cytoplasmic green fluorescent pattern that was mostly perinuclear (Fig. 5A). A similar pattern was observed when the Rlk-GFP fusion proteins were expressed in the Jurkat T-cell line (see Fig. 11). Furthermore, the ATG2 Rlk-GFP construct, expressing mainly the 83-kDa protein, showed an identical subcellular distribution (Fig. 5B). This pattern is characteristic of proteins that localize to endosomal membranes, and we have observed that Rlk partially colocalizes with Src, a molecule that specifically associates with endosomal membranes (14). Furthermore, we have observed that Rlk very closely colocalizes with the Src family member pp59^{FynT} (data not shown).

Surprisingly, in contrast to the findings with WT or the larger (83-kDa) form of Rlk-GFP, the shorter (77-kDa) protein produced from the ATG1 Rlk-GFP construct showed a diffuse nuclear pattern (Fig. 5C). Thus, the shorter form of Rlk is located in the nucleus when expressed in the absence of the larger form. These results suggest that the two forms of the Rlk protein can localize in different cellular compartments and perhaps may play distinct roles in T-cell signaling.

The two forms colocalize when coexpressed. Despite the nuclear localization of the p77^{Rlk} protein when expressed in isolation, nuclear staining was only weakly observed in HeLa cells expressing both the 83- and 77-kDa proteins from the WT

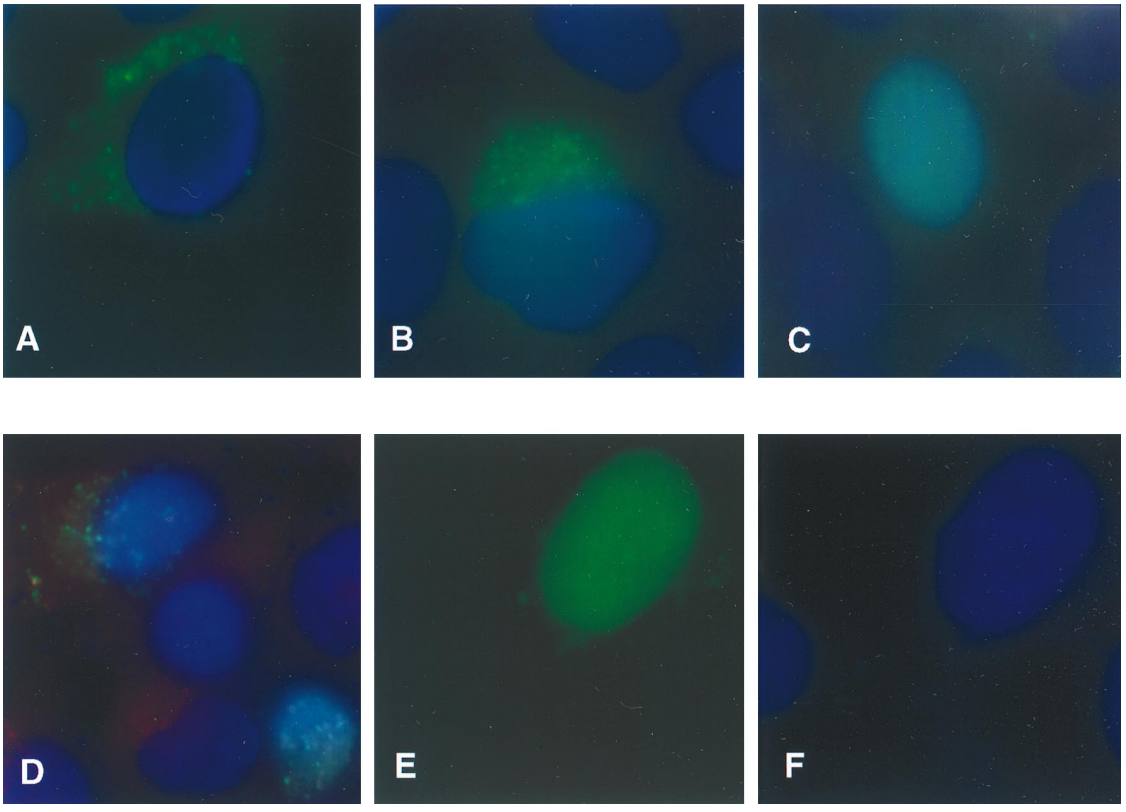

FIG. 5. Subcellular localization of the two forms of WT and mutant Rlk-GFP fusions. HeLa cells were transiently transfected with the following constructs, fixed, and stained with DAPI. (A) WT GFP-Rlk. (B) AUG2Rlk-GFP expressing only the long form. (C) AUG1Rlk-GFP expressing only the short form. (D) NLS mutant of the short form of Rlk-GFP (NLS-AUG1Rlk-GFP). (E and F) Cysteine mutant of the long form of Rlk (CMRlk-GFP) with fluorescein channel only (E) or DAPI only (F).

Rlk-GFP construct. The retention of the 77-kDa protein in the cytoplasmic compartment when both forms are coexpressed suggests that they may interact and thereby colocalize. To pursue this possibility, we differentially labeled the two forms by tagging the large form (ATG2-Rlk) at its carboxy terminus with blue fluorescent protein (BFP), a modified version of GFP. Because the fluorescent intensity of the BFP fusion protein is significantly lower than the GFP fusions, we performed these analyses with 293T cells, in which we obtain higher levels of protein expression than in HeLa cells.

In 293T cells, the larger form or both forms of Rlk together produce an intense globular pattern of fluorescence adjacent to, but lying outside of, the nucleus (Fig. 6B and data not shown). Cells expressing only the shorter form of Rlk (p77Rlk-GFP) show the characteristic nuclear pattern observed in HeLa cells (Fig. 6A). However, when coexpressed with p83Rlk-BFP, the characteristic nuclear pattern of p77Rlk-GFP was greatly reduced. Instead, p77Rlk-GFP was found in the same extranuclear region as the blue fluorescence pattern generated by p83Rlk-BFP (Fig. 6C and D). Although we have not been able to coprecipitate differentially tagged versions of Rlk, these results support the proposal that the two forms of the protein can colocalize when expressed together and that the presence of the larger Rlk isoform may recruit the smaller isoform to an extranuclear location.

The two forms display distinct localizations in T cells. T cells express *rlk* mRNA throughout development. We therefore asked whether we could find the two forms of the active enzyme in similar cell compartments in freshly harvested thymocytes. We fractionated thymocytes and examined immunoprecipitated Rlk protein by kinase assay. In these cells, we normally observed two forms of the Rlk kinase (Fig. 2A), which we also found in the cytoplasmic fraction (Fig. 7, lane 2). In contrast, the nuclear fraction is greatly enriched in the short form of the Rlk protein (Fig. 7, lane 1). These results suggest that endogenous Rlk can localize to different subcellular fractions and that at least a portion of the shorter species can be found in the nucleus. Furthermore, the detection of the short form in the nucleus in the absence of the long form strongly argues that the shorter phosphorylated protein observed in lymphocytes is also Rlk.

Determinants of protein localization. Inspection of the predicted amino acid sequence of Rlk revealed a cryptic bipartite nuclear localization signal (NLS) at residues 57 to 71 that is present in both species of RLK protein (Fig. 3) (9). To determine if this NLS causes nuclear localization of the shorter protein, we mutated the motif in the shorter GFP fusion construct (ATG1NLS-RlkGFP). The mutant protein failed to accumulate in the nucleus of either HeLa or 293T cells, instead being found in a granular pattern in the cytoplasm (Fig. 5D). Thus, this NLS is required for the nuclear localization of the shorter isoform of Rlk.

Since the longer form of the protein also contains this NLS, we reasoned that there must be some overriding feature that holds the longer form of the protein in the cytoplasm. One of the most distinctive features of the unique amino-terminal region of $p58^{Rlk}$ is the cysteine-rich region (Fig. 3). We therefore mutated three of the six cysteines in this region (CM) and examined the effects on subcellular localization. Remarkably, this mutation caused the majority of the protein to localize in

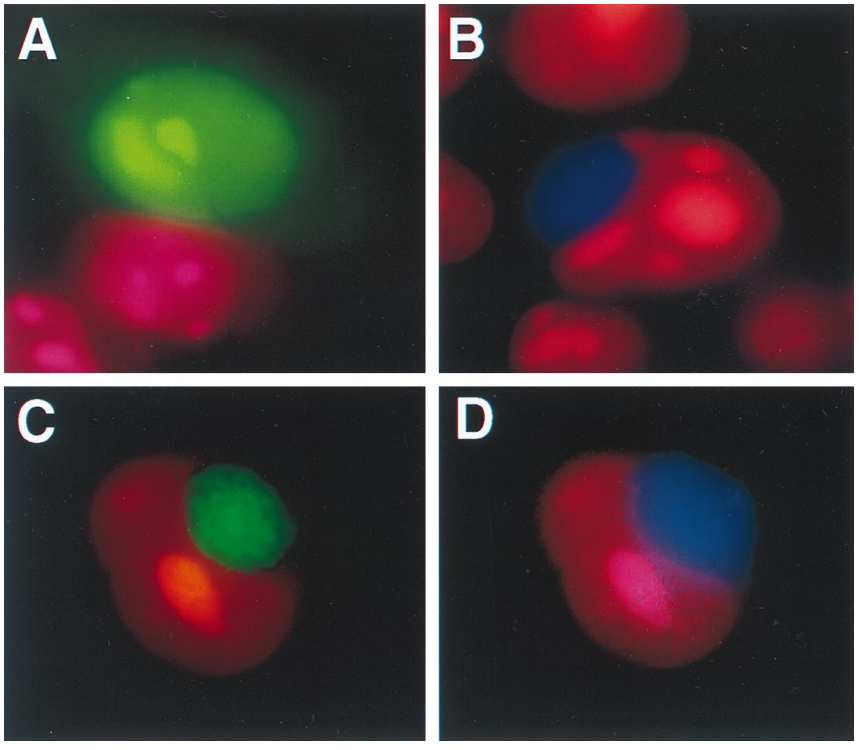

FIG. 6. The two forms of Rlk colocalize when coexpressed. 293T cells were transiently transfected with Rlk-GFP expression constructs, fixed, and counterstained with propidium iodide. (A) AUG1Rlk-GFP (short form). (B) AUG2Rlk-BFP (long form). (C and D) AUG2Rlk-BFP (long form) and AUG1Rlk-GFP (short form) cotransfected and visualized for GFP (C) or visualized for BFP (D). The colocalizations of the two forms of Rlk are indicated by arrows.

the nucleus (Fig. 5E and F). Thus, the NLS and the cysteine-rich motif play antagonistic roles in the subcellular localization of Rlk.

The cysteine motif mediates palmitoylation of Rlk. Cysteine string motifs have been found to be palmitoylated, a fatty acid modification that causes the association of proteins with certain membranous compartments (7, 8). We therefore examined whether the cysteines of Rlk could undergo fatty acid modification. 293T cells expressing WT Rlk-GFP, the cysteine mutant (CM) described above, or Fyn (an Src family member known to be palmitoylated) were metabolically labeled with [^{3}H]palmitate, and the appropriate proteins were immunoprecipitated from cell lysates. Incorporation of [^{3}H]palmitate, but not [^{3}H]myristate, is observed with the WT Rlk-GFP protein (Fig. 8A, lane 3, and data not shown). However, mutation of 3 of the 6 cysteines in the cysteine string motif (CM) dramatically decreased labeling of Rlk-GFP, consistent with alteration of the site of fatty acid labeling (Fig. 8A, lane 2). Boiling in 2-mercaptoethanol also reduced labeling of the WT protein (data not shown), suggesting that the mechanism of incorporation of fatty acid is consistent with an S acetylation such as palmitoylation. Thus, the cysteine string appears to mediate palmitoylation, and this modification may account for the ability of this motif to prevent nuclear localization of Rlk.

While two ^{3}H-labeled protein species are observed after immunoprecipitation with anti-Rlk serum in this experiment, we believe that the shorter species may be either an aberrant migration of some of the larger isoform under mild denaturing conditions or a coprecipitating protein, since it does not migrate at a position equivalent to the short Rlk isoform and was only observed in experiments using very mild reducing conditions. Furthermore, p77$^{Rlk\text{-}GFP}$ is not labeled with [^{3}H]palmitate when expressed in isolation or as part of the CM mutant (Fig. 8A, lane 2, and data not shown).

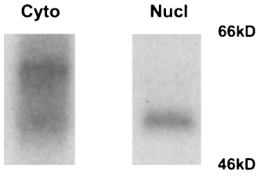

FIG. 7. Subcellular fractionation of murine thymocytes. Cells were fractionated as described in the text, and the nuclear and cytoplasmic fractions from 6×10^7 cells were immunoprecipitated and analyzed by kinase assay. Nucl, nuclear pellet; Cyto, S100 supernatant.

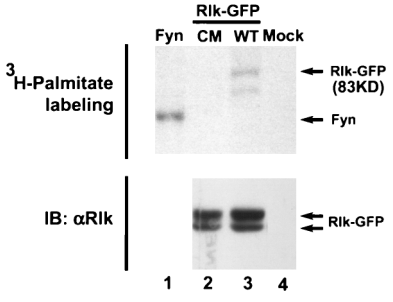

FIG. 8. WT Rlk is modified by palmitoylation. Mutation of the cysteine string abolishes [^{3}H]palmitate labeling. 293T cells were transfected with cDNAs encoding Fyn (positive control, lane 1), a cysteine mutant of Rlk-GFP (lane 2), WT Rlk (lane 3), or control vector alone (lane 4). Twenty-four hours after transfection, cells were labeled with [^{3}H]palmitate for 2 h, washed, and lysed, and Rlk or Fyn was immunoprecipitated as described in the text. (Top) Samples were analyzed by SDS–10% PAGE and visualized by fluorography. (Bottom) Immunoblot (IB) for Rlk.

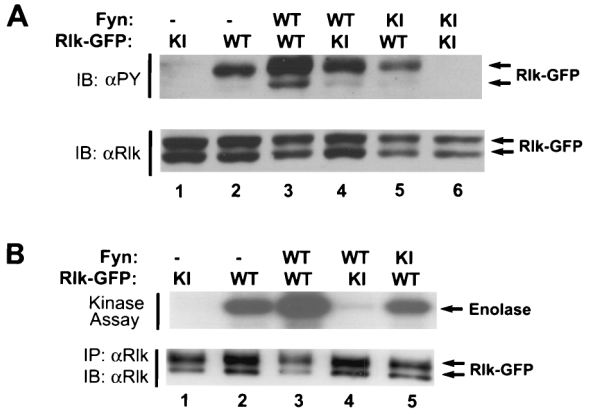

FIG. 9. Tyrosine phosphorylation and activation of Rlk kinase upon coexpression with Fyn in 293T cells. (A) 293T cells were transfected with Rlk-GFP fusion and FynT expression constructs, followed by cell lysis at 24 h. Equal amounts of detergent-soluble lysates were resolved by SDS-PAGE and subjected to antiphosphotyrosine (4G10) (top) or anti-Rlk (bottom) immunoblotting (IB). (B) Immune complex kinase assays. Cells expressing Rlk-GFP fusion proteins alone or with Fyn were lysed and immunoprecipitated with anti-Rlk. Immune complexes were washed and subjected to an in vitro kinase assay with [γ-^{32}P]ATP and acid-denatured enolase as an exogenous substrate. Phosphorylated proteins were resolved by SDS-PAGE and detected by autoradiography. (Top) In vitro kinase activity on enolase. (Bottom) anti-Rlk. Equivalent expression of Fyn was confirmed by immunoblotting with anti-Fyn (data not shown). WT, wild type (kinase active); KI, kinase inactive.

Rlk is activated by Src family members. The above data suggest that Rlk, unlike the other Btk family kinases, has a distinct regulation of localization, consistent with its lack of a PH domain. Nonetheless, other features of Rlk closely resemble the Btk kinases. In particular, Rlk shares the common SH2, SH3, and kinase domains, as well as a proline-rich sequence. This proline-rich region has been shown in vitro to mediate an interaction with the SH3 domains of certain Src family kinases in vitro. Similarly, we have observed an in vitro interaction with the SH3 domains of the Src family members Fyn, Hck, and Lyn (3a).

Src family members have been shown to phosphorylate Btk, Itk, and Tec (10, 26). This phosphorylation on a tyrosine in the activation loop of the kinase domain has further been demonstrated to increase the kinase activity of Btk and Itk and to cause an autophosphorylation of a tyrosine in the SH3 domain of Btk. Since Rlk possesses homologous sequences and shows similar binding of Src family SH3 domains in vitro, we asked whether Rlk may be similarly activated.

We therefore coexpressed Rlk and the Src family member Fyn in 293T cells and examined Rlk phosphorylation and kinase activity. Since Rlk and Src family kinases are similar in electrophoretic mobility, we took advantage of our Rlk-GFP fusion constructs for these experiments. Coexpression of Rlk-GFP with Fyn led to an increase in the amount of phosphotyrosine in WT Rlk-GFP (Fig. 9A, lanes 1 and 2). In contrast, no significant increase in phosphotyrosine is observed upon coexpression of WT Rlk with a kinase-inactive Fyn (Fig. 9A, lane 5). Kinase-inactive Rlk (K299R) showed virtually no evidence of tyrosine phosphorylation unless coexpressed with kinase-active Fyn (Fig. 9; compare lanes 1, 4, and 6). Because tyrosine phosphorylation of kinase-inactive Rlk expressed with Fyn is markedly reduced relative to WT Rlk expressed with Fyn (Fig. 9, lanes 3 and 4), maximal tyrosine phosphorylation of Rlk appears to require both Rlk and Fyn kinase activities, consistent with an increase in Rlk autophosphorylation activity upon phosphorylation by Fyn.

To assess the activation status of Rlk-GFP, we performed in vitro kinase assays on immunoprecipitated Rlk, using enolase as a substrate (Fig. 9B). Coexpression of Rlk with WT Fyn augmented the kinase activity of Rlk by four-to sixfold on the exogenous substrate enolase. Under these conditions, the increase in enolase phosphorylation appears to be specific for Rlk and not derived from the small amount of coimmunoprecipitated Fyn, since there was no significant phosphorylation of enolase when kinase-inactive Rlk was expressed with WT Fyn (Fig. 9B, lane 4). Furthermore, a similar increase in Rlk autophosphorylation activity was observed (data not shown). In contrast, Rlk kinase activity did not increase when Rlk was coexpressed with kinase-inactive Fyn (Fig. 9B, lane 5). We have also found that Rlk coexpression with Fyn does not appear to increase phosphorylation or kinase activity of Fyn.

Finally, we noted that the shorter form of Rlk is not efficiently phosphorylated by Src family kinases, consistent with its potential for localization in a different subcellular compartment (Fig. 9A, lane 3). Expression of only the short form of Rlk with Fyn corroborated this observation (data not shown). Accordingly, when expressed alone, the shorter form of Rlk also had a lower specific kinase activity (data not shown).

Activation by Src family kinases is independent of PI 3-kinase activity. It has been suggested that activation of Itk and Btk by Src kinases requires a translocation to the membrane mediated by the interaction between the PH domain and the products of PI 3-kinase (2). The products of PI 3-kinase have been found to interact with PH domains of Btk and Itk, and it has recently been demonstrated that phosphorylation and activation of Itk by Src family kinases is dependent on the activity of PI 3-kinase. Either inhibitors of PI 3-kinase activity or mutation of the PH domain will decrease activation of Itk by Src family kinases (2). Furthermore, activation of BTK by Src can be potentiated by overexpression of PI 3-kinase (19).

Since Rlk does not contain a PH domain, we investigated whether activation of Rlk by Src family kinases also required PI 3-kinase activity. We observed no decrease in the activation of Rlk by Fyn when cells were incubated with Wortmannin or Ly294002, two inhibitors of PI 3-kinase that greatly reduce activation of Itk under the same conditions (Fig. 10). Thus, activation of Rlk by Src family members may occur by a mechanism distinct from that used by Itk and Btk, consistent with our observations that Rlk has a different means of membrane association.

Rlk can be activated by TCR signaling in Jurkat cells. The ability of Src family kinases to activate Rlk suggests that Rlk

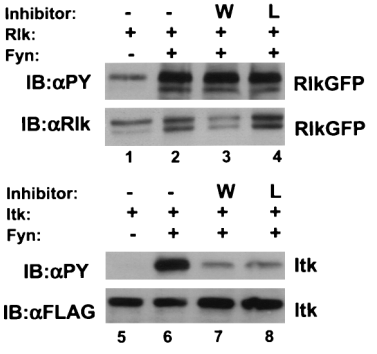

FIG. 10. Rlk activation by Fyn is not affected by inhibitors of PI 3-kinase. (Top) Cells were transfected with constructs expressing either Rlk alone or Rlk plus Fyn. Twenty-four hours after transfection, cells were split equally and treated 24 h later with either dimethyl sulfoxide (DMSO) (lanes 1 and 2), 1 mM Wortmannin (lane 3), or 100 mM Ly294002 (lane 4). After 30 min, cells were lysed, resolved by SDS-PAGE, and examined by Western blotting with antiphosphotyrosine (top row) or anti-Rlk (bottom row). (Bottom) Cells were transfected with constructs expressing either Itk-FLAG alone or Itk-FLAG plus Fyn and treated as above with either DMSO (lanes 5 and 6), 1 mM Wortmannin (lane 7), or 100 mM Ly294002 (lane 8). Western blotting was performed with antiphosphotyrosine (top row) or anti-FLAG (bottom row).

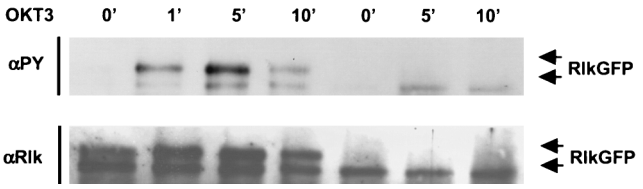

FIG. 11. Tyrosine phosphorylation of Rlk-GFP in Jurkat cells. Cells were electroporated with either WT Rlk-GFP or AUG2Rlk-GFP expressing only the short form of Rlk. Twenty-four hours later, cells were stimulated with anti-CD3 antibody OKT3 for the indicated times (in minutes). Cells were lysed and Rlk was immunoprecipitated. Immunoprecipitated Rlk was immunoblotted with antiphosphotyrosine (4G10) (top) or anti-Rlk (bottom).

may be activated downstream of Src family kinases by TCR signaling, in a fashion analogous to Btk in B-cell-receptor signaling. To examine Rlk activation in T-cell signaling, we again took advantage of our Rlk-GFP constructs and expressed them in the Jurkat T-cell lymphoma line, a strategy that allowed us to bypass technical difficulties associated with comigration of Rlk with the heavy chain of our anti-Rlk antiserum. Activation of Jurkat cells by stimulation with the OKT3 antibody directed against the CD3 component of the TCR induced rapid tyrosine phosphorylation of Rlk-GFP (Fig. 11, lanes 1 to 4). In contrast, the shorter form of Rlk was not efficiently phosphorylated in response to OKT3 (Fig. 11, lanes 5 to 7), again supporting hypothetically different roles for the two forms of Rlk. Thus, we conclude the longer form of Rlk is most likely to be the principle form involved in signaling from cell surface receptors in T cells.

Activation of Jurkat cells alters the subcellular localization of Rlk. To examine whether T-cell activation affects the subcellular distribution of Rlk, we again expressed Rlk-GFP transiently in Jurkat cells and stimulated them either through the TCR with the OKT3 antibody or with PMA and ionomycin. Full-length Rlk-GFP gave a vesicular type of localization outside the nucleus in Jurkat cells, consistent with that observed in HeLa cells (Fig. 12A). Localization of the short form of Rlk was less clear in Jurkat cells, suggesting both a nuclear and nonnuclear localization (data not shown). However, long-term activation with either PMA and ionomycin or with anti CD3 antibodies led to an apparent localization of either full-length Rlk-GFP or the short form (AUG1Rlk-GFP) in the nucleus (Fig. 12B and C and data not shown). To investigate this subcellular trafficking in further detail, we examined live Jurkat cells expressing the Rlk-GFP constructs at a range of times post-TCR stimulation. While initial stimulation did not appreciably alter the pattern of localization, stimulation for 10 to 15 min revealed two new distinct compartments. A subpopulation of Rlk was observed to migrate to the plasma cell membrane, consistent with activation by the TCR. Additionally, a second population of the protein was observed in the nucleus. Over the next 30 to 60 min the membrane fraction disappeared, while the nuclear component remained. While the function of this nuclear fraction remains unclear, these results further demonstrate a nuclear localization for Rlk in lymphocytes, which may be important for unique signaling pathways involving Rlk.

DISCUSSION

By several criteria, Rlk appears to be a member of the Btk family of kinases, yet significant differences exist between Rlk and the other kinases in this family. In this report, we show that the distinct molecular features of Rlk confer unique biological properties on the kinase that may be important for its normal cellular function. We demonstrate here that *rlk*/*txk* encodes two proteins generated by the alternative initiation of translation from a single mRNA. In the case of murine Rlk, most or all of the smaller isoform is generated from an internal start site located 55 residues downstream of the upstream AUG. This smaller form contains the catalytic, SH2, and SH3 domains, as well as the proline-rich motif found in common with other BTK family kinases; however, it lacks much of the unique amino-terminal sequence, including a distinct cysteine string motif, present in the larger 58-kDa isoform. We further demonstrate that the two Rlk isoforms have distinct properties, including subcellular locations and fatty acid modification, and that the cysteine string motif helps dictate both palmitoylation and subcellular localization.

Determinants of the subcellular localization of Rlk. Alternative initiation sites can affect the subcellular location and modification of proteins. For example, the 59-kDa isoform of Hck is both palmitoylated and myristoylated and is associated with cellular membranes, most notably caveolae, whereas the 61-kDa isoform is not palmitoylated and not associated with caveolae (28). In Rlk, two motifs help determine its subcellular location. The cysteine string motif is important for perinuclear localization and can override a bipartite NLS, which is required for nuclear targeting of the short form. Hence, lacking the cysteine-rich motif, the 52-kDa form is located in the nucleus when expressed in isolation.

The cysteine string motif found in the amino terminus of Rlk is unique among tyrosine kinases. Other cysteine string proteins include synaptotagmin and GAIP (G-alpha interacting protein), molecules implicated in vesicular transport and in the presynaptic Ca^{2+} influx related to synaptic vesicular release (3, 5, 23, 34). In this regard, it is interesting that the phenotype of $rlk^{-/-}$ $itk^{-/-}$ mice includes a specific decrease in Ca^{2+} influx in response to TCR-based signaling (unpublished data).

Cysteine residues near the amino termini of signaling molecules, including the cysteine string motifs, are important for palmitoylation, a posttranslational lipid modification in which palmitate is linked to cysteine via a labile thioester bond (7, 27). We found that Rlk can be labeled by [^{3}H]palmitate and not by [^{3}H]myristate (Fig. 9 and data not shown) and that mutation of the cysteines eliminates palmitoylation. Many signaling molecules, including the Src family kinases Lck, Fyn, and Hck, are also palmitoylated, and this modification has been shown to affect membrane association, the ability to interact with GPI-linked proteins on the cell surface, and localization in glycolipid-enriched regions of the membrane (GEMs or RAFTs) (31). Notably, these regions are insoluble in nonionic detergents—a characteristic of the larger form of Rlk. Rlk coimmunoprecipitates and colocalizes with Fyn (data not shown), a palmitoylated kinase associated with these membrane compartments. Proper palmitoylation may be required for signal transduction of these molecules, as has been shown for Lck in TCR signaling (13). Furthermore, palmitoylation can be a dynamic and reversible process with functional implications. For example, palmitoylation of G protein subunits can be modulated in response to receptor activation, thereby leading to changes in G protein subcellular localization and receptor sensitization (5, 33). It is of interest that after prolonged stimulation of Jurkat T cells, we observed a nuclear localization of Rlk-GFP. The functional consequences of changes in palmitoylation and subcellular localization of Rlk during TCR-based signaling are under further investigation.

Activation of Rlk. We demonstrate here that activation of the TCR via OKT3 can lead to increased phosphorylation of Rlk transfected into Jurkat T cells. Coexpression of Rlk with Src family kinases in heterologous cells also leads to increased phosphorylation of the full-length Rlk and activation of the

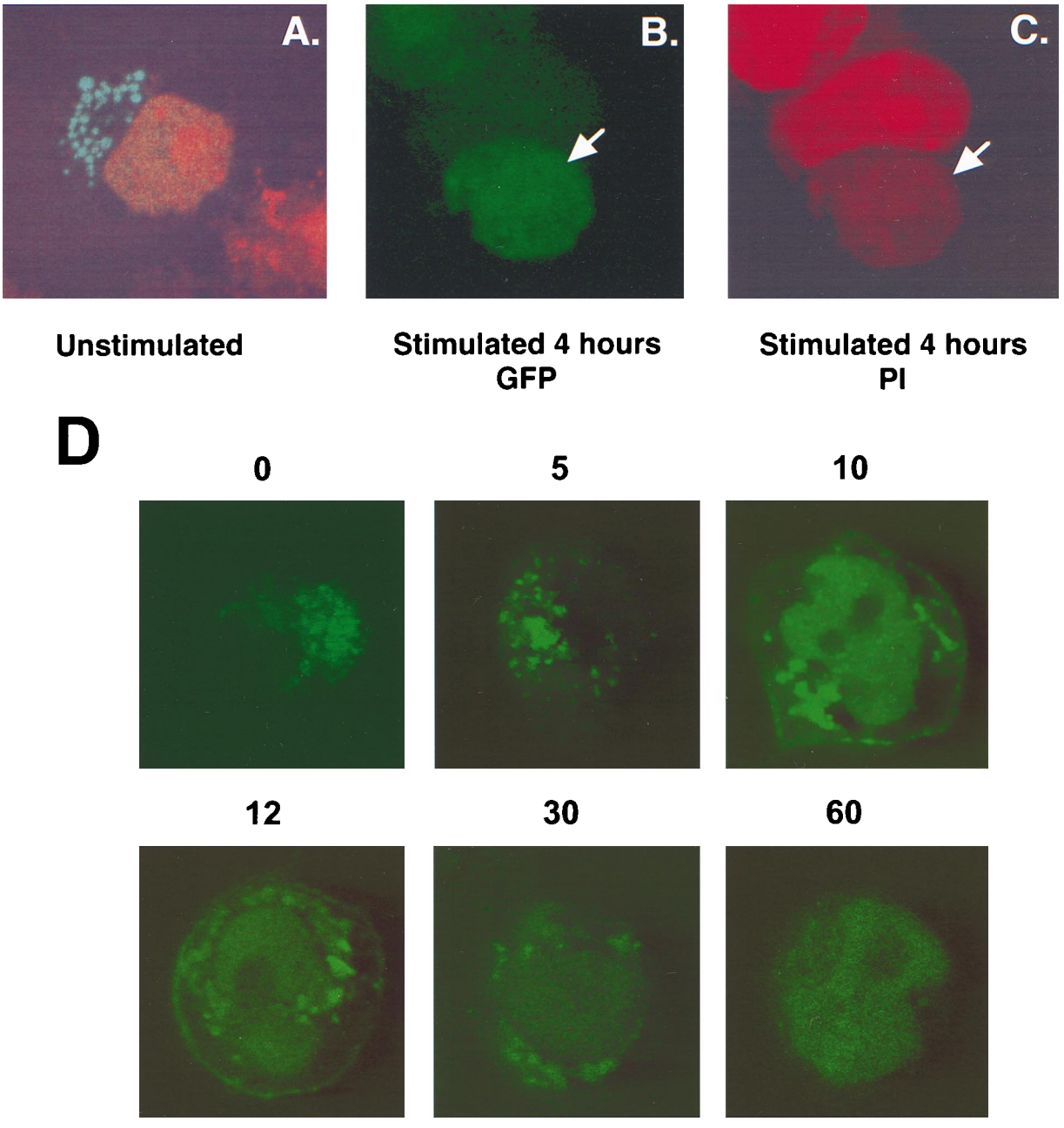

FIG. 12. Activation of Jurkat cells changes the subcellular localization of Rlk. Cells were electroporated with WT Rlk-GFP and stimulated 24 h later with either OKT3 or PMA and ionomycin, counterstained with propidium iodide, and examined by confocal microscopy. (A) Unstimulated cells. (B) Stimulated cells, fluorescein channel. (C) Same as panel B, with rhodamine channel for visualizing propidium iodide. (D) Time course of localization of Rlk-GFP after TCR stimulation. Cells were visualized live at the indicated times (in minutes) after treatment with anti-CD3.

Rlk kinase, suggesting that Rlk may be a downstream effector of Src family kinases in TCR signaling. However, while Rlk is phosphorylated and activated in a fashion similar to the other Btk kinases, there are marked differences between these kinases, most notably the lack of a PH domain in Rlk. A recent model suggests that membrane association of Itk and Btk results from the interaction of their PH domains with products of PI 3-kinase, thereby allowing activation by Src family kinases. Accordingly, activation of Itk by Src kinases is inhibited by Wortmannin and Ly294002 (2, 19). This is not observed for Rlk and suggests that interactions of Rlk with Src family kinases is distinct from the other Btk kinases. It is of interest that the full-length form of Rlk has a higher basal level of tyrosine phosphorylation and kinase activity than Itk when expressed in heterologous cells (Fig. 10), which could be the result of different upstream interactions and regulation of localization. Moreover, we can reproducibly coimmunoprecipitate Rlk and Fyn, whereas we and others have been unable to coprecipitate Itk and Btk with members of the Src family (data not shown), implying that there is a direct interaction between Rlk and the Src kinases.

In addition to properties that distinguish Rlk from the other Btk family kinases, differences exist between the two forms of Rlk, including their different potential subcellular localizations. Furthermore, phosphorylation of the short form of Rlk is less robust than for full-length Rlk. We have also observed that expression of the full-length form, but not the short form,

increases JNK activity in 293T cells (3b). The conservation of two Rlk/TXK isoforms in mouse and human, in concert with the different properties of these proteins, suggests distinct functions for the two forms of Rlk in T-cell physiology. In particular, the stronger activation of the long form of Rlk and the trafficking of two distinct subpopulations of Rlk to either the plasma membrane or the nucleus after TCR stimulation suggests that they may have different functions in T-cell signaling.

Our data provide the first evidence of a signaling pathway that may activate the Rlk kinase downstream from the TCR. The phosphorylation of Rlk by Src family members, furthermore, suggests that Rlk, like other Btk family kinases, functions downstream of Src family kinases in signal transduction pathways from antigen receptors. Preliminary evidence from gene-targeted mice supports these data and suggests that Rlk may synergize with Itk in signaling from the TCR, and deficiency of both kinases leads to profound defects in cytokine gene transcription and T-cell activation (unpublished data). Thus, Rlk together with Itk may occupy a position in TCR signaling pathways similar to that of Btk in B-cell-receptor signaling. We have also demonstrated that Rlk can augment activation of an IL-2 reporter construct upon signaling from the TCR (36). In this and other assay systems, the truncated (short) form of Rlk has been found to be less active. As evidence of downstream targets and pathways emerges, the distinct functions of the two forms of this kinase in T-cell signaling may be further understood.

ACKNOWLEDGMENTS

J.D. and M.C. contributed equally to this work.

J.D. was a Howard Hughes Medical Institute—NIH Research Scholar. P.L.S. was a Special Fellow of the Leukemia Society of America.

We thank G. Gaitanaris, G. Pavlakis, S. Gutkind, and D. Littman for plasmid constructs, as well as L. Matis for the original Rlk cDNA clone. We also thank M. Tomlinson for the generous gift of anti-human TXK antisera, A. Weissman for the gift of purified OKT3, and E. Schrock, C. Hemphill, and B. Thomas for assistance with confocal microscopy.

REFERENCES

1. **August, A., S. Gibson, Y. Kawakami, T. Kawakami, G. B. Mills, and B. Dupont.** 1994. CD28 is associated with and induces the immediate tyrosine phosphorylation and activation of the Tec family kinase ITK/EMT in the human Jurkat leukemic T-cell line. Proc. Natl. Acad. Sci. USA **91:**9347–9351.
2. **August, A., A. Sadra, B. Dupont, and H. Hanafusa.** 1997. Src-induced activation of inducible T cell kinase (ITK) requires phosphatidylinositol 3-kinase activity and the Pleckstrin homology domain of inducible T cell kinase. Proc. Natl. Acad. Sci. USA **94:**11227–11232.
3. **Braun, J. E., and R. H. Scheller.** 1995. Cysteine string protein, a DnaJ family member, is present on diverse secretory vesicles. Neuropharmacology **34:** 1361–1369.

3a. **Cheng, G., M. Chamorro, and P. L. Schwartzberg.** Unpublished observations.

3b. **Debnath, J.** Unpublished observations.

4. **Desiderio, S., and J. D. Siliciano.** 1994. The Itk/Btk/Tec family of protein-tyrosine kinases. Chem. Immunol. **59:**191–210.
5. **De Vries, L., E. Elenko, L. Hubler, T. L. Jones, and M. G. Farquhar.** 1996. GAIP is membrane-anchored by palmitoylation and interacts with the activated (GTP-bound) form of G alpha i subunits. Proc. Natl. Acad. Sci. USA **93:**15203–15208.
6. **Gibson, S., A. August, Y. Kawakami, T. Kawakami, B. Dupont, and G. B. Mills.** 1996. The EMT/ITK/TSK (EMT) tyrosine kinase is activated during TCR signaling: LCK is required for optimal activation of EMT. J. Immunol. **156:**2716–2722.
7. **Gundersen, C. B., A. Mastrogiacomo, K. Faull, and J. A. Umbach.** 1994. Extensive lipidation of a Torpedo cysteine string protein. J. Biol. Chem. **269:**19197–19199.
8. **Gundersen, C. B., A. Mastrogiacomo, and J. A. Umbach.** 1995. Cysteine-string proteins as templates for membrane fusion: models of synaptic vesicle exocytosis. J. Theor. Biol. **172:**269–277.
9. **Haire, R. N., Y. Ohta, J. E. Lewis, S. M. Fu, P. Kroisel, and G. W. Litman.** 1994. TXK, a novel human tyrosine kinase expressed in T cells, shares sequence identity with Tec family kinases and maps to 4p12. Hum. Mol. Genet. **3:**897–901.
10. **Heyeck, S. D., H. M. Wilcox, S. C. Bunnell, and L. J. Berg.** 1997. Lck phosphorylates the activation loop tyrosine of the Itk kinase domain and activates Itk kinase activity. J. Biol. Chem. **272:**25401–25408.
11. **Horton, R. M.** 1997. In vitro recombination and mutagenesis of DNA. SOEing together tailor-made genes. Methods Mol. Biol. **67:**141–149.
12. **Hu, Q., D. Davidson, P. L. Schwartzberg, F. Macchiarini, M. J. Lenardo, J. A. Bluestone, and L. A. Matis.** 1995. Identification of Rlk, a novel protein tyrosine kinase with predominant expression in the T cell lineage. J. Biol. Chem. **270:**1928–1934.
13. **Kabouridis, P. S., A. I. Magee, and S. C. Ley.** 1997. S-acylation of LCK protein tyrosine kinase is essential for its signalling function in T lymphocytes. EMBO J. **16:**4983–4998.
14. **Kaplan, K. B., J. R. Swedlow, H. E. Varmus, and D. O. Morgan.** 1992. Association of $p60^{c\text{-}src}$ with endosomal membranes in mammalian fibroblasts. J. Cell Biol. **118:**321–333.
15. **Kawakami, Y., L. Yao, T. Miura, S. Tsukada, O. N. Witte, and T. Kawakami.** 1994. Tyrosine phosphorylation and activation of Bruton tyrosine kinase upon FcεRI cross-linking. Mol. Cell. Biol. **14:**5108–5113.
16. **Kawakami, Y., L. Yao, M. Tashiro, S. Gibson, G. B. Mills, and T. Kawakami.** 1995. Activation and interaction with protein kinase C of a cytoplasmic tyrosine kinase, Itk/Tsk/Emt, on Fc epsilon RI cross-linking on mast cells. J. Immunol. **155:**3556–3562.
17. **Kozak, M.** 1992. Regulation of translation in eukaryotic systems. Annu. Rev. Cell Biol. **8:**197–225.
18. **Kozak, M.** 1991. Structural features in eukaryotic mRNAs that modulate the initiation of translation. J. Biol. Chem. **266:**19867–19870.
19. **Li, Z., M. Wahl, A. Eguino, L. Stephens, P. Hawkins, and O. Witte.** 1997. Phosphotidylinositol 3-kinase-γ activates Bruton's tyrosine kinase in concert with Src family kinases. Proc. Natl. Acad. Sci. USA **94:**13820–13825.
20. **Liao, X. C., and D. R. Littman.** 1995. Altered T cell receptor signaling and disrupted T cell development in mice lacking Itk. Immunity **3:**757–769.
21. **Liu, K. Q., S. C. Bunnell, C. B. Gurniak, and L. J. Berg.** 1998. T cell receptor-initiated calcium release is uncoupled from capacitative calcium entry in Itk-deficient T cells. J. Exp. Med. **187:**1721–1727.
22. **Mahajan, S., J. Fargnoli, A. L. Burkhardt, S. A. Kut, S. J. Saouaf, and J. B. Bolen.** 1995. Src family protein tyrosine kinases induce autoactivation of Bruton's tyrosine kinase. Mol. Cell. Biol. **15:**5304–5311.
23. **Mastrogiacomo, A., S. M. Parsons, G. A. Zampighi, D. J. Jenden, J. A. Umbach, and C. B. Gundersen.** 1994. Cysteine string proteins: a potential link between synaptic vesicles and presynaptic Ca2+ channels. Science **263:** 981–982.
24. **Matsuda, T., M. Takahashi-Tezuka, T. Fukada, Y. Okuyama, Y. Fujitani, S. Tsukada, H. Mano, H. Hirai, O. N. Witte, and T. Hirano.** 1995. Association and activation of Btk and Tec tyrosine kinases by gp130, a signal transducer of the interleukin-6 family of cytokines. Blood **85:**627–633.
25. **Pear, W. S., G. P. Nolan, M. L. Scott, and D. Baltimore.** 1993. Production of high-titer helper-free retroviruses by transient transfection. Proc. Natl. Acad. Sci. USA **90:**8392–8396.
26. **Rawlings, D. J., A. M. Scharenberg, H. Park, M. I. Wahl, S. Lin, R. M. Kato, A. C. Fluckiger, O. N. Witte, and J. P. Kinet.** 1996. Activation of BTK by a phosphorylation mechanism initiated by SRC family kinases. Science **271:** 822–825.
27. **Resh, M. D.** 1994. Myristylation and palmitylation of Src family members: the fats of the matter. Cell **76:**411–413.
28. **Robbins, S. M., N. A. Quintrell, and J. M. Bishop.** 1995. Myristoylation and differential palmitoylation of the *HCK* protein-tyrosine kinases govern their attachment to membranes and association with caveolae. Mol. Cell. Biol. **15:**3507–3515.
29. **Saouaf, S. J., S. Mahajan, R. B. Rowley, S. A. Kut, J. Fargnoli, A. L. Burkhardt, S. Tsukada, O. N. Witte, and J. B. Bolen.** 1994. Temporal differences in the activation of three classes of non-transmembrane protein tyrosine kinases following B-cell antigen receptor surface engagement. Proc. Natl. Acad. Sci. USA **91:**9524–9528.
30. **Sato, S., T. Katagiri, S. Takaki, Y. Kikuchi, Y. Hitoshi, S. Yonehara, S. Tsukada, D. Kitamura, T. Watanabe, O. Witte, et al.** 1994. IL-5 receptor-mediated tyrosine phosphorylation of SH2/SH3-containing proteins and activation of Bruton's tyrosine and Janus 2 kinases. J. Exp. Med. **180:**2101–2111.

30a. **Schwartzberg, P. L.** Unpublished observations.

31. **Simons, K., and E. Ikonen.** 1997. Functional rafts in cell membranes. Nature **387:**569–572.
32. **Sommers, C. L., K. Huang, E. W. Shores, A. Grinberg, D. A. Charlick, C. A. Kozak, and P. E. Love.** 1995. Murine txk: a protein tyrosine kinase gene regulated by T cell activation. Oncogene **11:**245–251.
33. **Tu, Y., J. Wang, and E. M. Ross.** 1997. Inhibition of brain Gz GAP and other RGS proteins by palmitoylation of G protein alpha subunits. Science **278:** 1132–1135.
34. **Umbach, J. A., A. Mastrogiacomo, and C. B. Gundersen.** 1995. Cysteine string proteins and presynaptic function. J. Physiol. (Paris) **89:**95–101.
35. **Weiss, A., and D. R. Littman.** 1994. Signal transduction by lymphocyte antigen receptors. Cell **76:**263–274.